CORA Cork Open Research Archive
Cartlann Taighde Oscailte Chorcaí

Title	Emerging meso- and macroscales from synchronization of adaptive networks
Authors	Gutierrez, R.;Amann, Andreas;Assenza, S.;Gomez-Gardenes, J.;Latora, V.;Boccaletti, S.
Publication date	2011
Original Citation	Gutiérrez, R., Amann, A., Assenza, S., Gómez-Gardeñes, J., Latora, V. and Boccaletti, S. (2011) 'Emerging meso- and macroscales from synchronization of adaptive networks', Physical Review Letters, 107(23), 234103 (5pp). doi: 10.1103/PhysRevLett.107.234103
Type of publication	Article (peer-reviewed)
Link to publisher's version	https://journals.aps.org/prl/abstract/10.1103/PhysRevLett.107.234103 - 10.1103/PhysRevLett.107.234103
Rights	© 2011, American Physical Society
Download date	2026-11-06 11:58:04
Item downloaded from	https://hdl.handle.net/10468/4626

UCC
University College Cork, Ireland
Coláiste na hOllscoile Corcaigh

Emerging Meso- and Macroscales from Synchronization of Adaptive Networks

R. Gutiérrez,[1] A. Amann,[2] S. Assenza,[3] J. Gómez-Gardeñes,[4] V. Latora,[5] and S. Boccaletti[1]

[1]*Centre for Biomedical Technology, Technical University of Madrid, Pozuelo de Alarcón, 28223 Madrid, Spain*
[2]*School of Mathematical Sciences and Tyndall National Institute, University College Cork, Cork, Ireland*
[3]*Laboratorio sui Sistemi Complessi, Scuola Superiore di Catania, 95123 Catania, Italy and Laboratoire de Biophysique Statistique, Ecole Polytechnique Fédérale de Lausanne, CH-1015 Lausanne, Switzerland*
[4]*Institute for Biocomputation and Physics of Complex Systems (BIFI), University of Zaragoza, 50018 Zaragoza, Spain and Department of Condensed Matter Physics, University of Zaragoza, 50009 Zaragoza, Spain*
[5]*Dipartimento di Fisica e Astronomia, Università di Catania and INFN, Via S. Sofia, 64, 95123 Catania, Italy and Laboratorio sui Sistemi Complessi, Scuola Superiore di Catania, Universitá di Catania, 95123 Catania, Italy*

(Received 26 July 2011; published 30 November 2011)

We consider a set of interacting phase oscillators, with a coupling between synchronized nodes adaptively reinforced, and the constraint of a limited resource for a node to establish connections with the other units of the network. We show that such a competitive mechanism leads to the emergence of a rich modular structure underlying cluster synchronization, and to a scale-free distribution for the connection strengths of the units.

DOI: 10.1103/PhysRevLett.107.234103 PACS numbers: 05.45.Xt, 89.75.Hc

From interacting populations of animals to the cells of our body, many social, biological, and man-made systems can be represented as an ensemble of dynamical units coupled via complex architectures. The analysis of such systems has revealed that, despite the intrinsic differences, their structure is characterized by two unifying properties [1]: (i) a power law (scale-free) scaling in the network connectivity, and (ii) the presence of modules (community structures) at a mesoscopic scale. While no model exists yet able to reproduce at once these two features, their interplay is believed to be the basis of the systems' general functioning and performance.

In this Letter, we consider a generic model of networked phase oscillators, with an initial topology set up by a random assignment of neighbors. The coupling is directed and time varying, and the temporal evolution of the link weights is coupled to the dynamics of the oscillators. Numerical and analytical studies of the synchronization properties (both at a local and a global scale) allow us to conclude that a competitive adaptive mechanism not only enhances synchronization, but also yields the simultaneous emergence of a mesoscale of communities and a scale-free distribution in the connection weights. The mechanism through which the dynamics reshapes the network structure is governed by the competition between the following two principles: (a) the connections between synchronized units are enhanced; (b) the available resources per unit to sustain interactions with the rest of the ensemble are limited. Principle (a) is known to be relevant in neuronal plasticity, or spreading in sociology, under the terms of Hebbian learning [2] and homophily [3], respectively. The limitation in the associative capacity given by principle (b) is known to play a relevant role in neuroscience under the term homeostasis [4], while in social systems it is related to the Dunbar's number [5]. Neuroscience is, indeed, the field in which more efforts have been put into elucidating the role of adaptive mechanisms, and various studies on neuronal plasticity (based on specific forms of competitive adaptation that underlie memory and learning abilities) reported the emergence of one or the other of the main features that we will describe in our model. Examples are the experimental and numerical evidence of an enhancement of synchronization of neurons originally spiking at different rates [6], and the emergence of synchronized clusters of different sizes allowing for the storing of information [7].

The model consists of a Kuramoto type ensemble of N phase oscillators. Each node i is characterized by its phase φ_i, and interacts with K randomly selected neighboring units, that form the set $\mathcal{N}_i$. The dynamics of the network is given by

$$\dot{\varphi}_i = \omega_i + \lambda \sum_{j \in \mathcal{N}_i} w_{ij} \sin(\varphi_j - \varphi_i), \tag{1}$$

where ω_i are randomly assigned natural frequencies (uniformly distributed in $[-\pi, \pi]$), w_{ij} is the weight of the link connecting node j to i, and λ is a coupling strength. Initially, the phases are randomly selected in the interval $[-\pi, \pi]$, and all weights are set to $1/K$. The adaptive evolution of the weights w_{ij} in Eq. (1) is governed by

$$\dot{w}_{ij} = p_{ij} - \Big(\sum_{k \in \mathcal{N}_i} p_{ik} \Big) w_{ij}, \tag{2}$$

where the quantity p_{ij} denotes the average phase correlation between oscillators i and j over a characteristic memory time T, and is defined as

 © 2011 American Physical Society

$$p_{ij} = \frac{1}{T}\left|\int_{-\infty}^{t} e^{(-(t-t')/T)} e^{i[\varphi_i(t')-\varphi_j(t')]} dt'\right|. \quad (3)$$

It follows from (2) that the normalization condition $\sum_{j\in\mathcal{N}_i} w_{ij} = 1$ holds at all times; i.e., the sum of the weights of all incoming connections at each node is conserved. Notice that the first and the second term in the right-hand side of Eq. (2) account, respectively, for homophily and homeostasis. Global synchronization can be quantified through the time dependent Kuramoto order parameter $r(t) = \frac{1}{N}\left|\sum_{i=1}^{N} e^{i\varphi_i(t)}\right|$ [8]. For a generic choice of λ and T, our results consistently show that the system evolves into an asymptotic state after some time t_s, where the weights w_{ij} take well-defined values, with small and stationary fluctuations. Then, we can define a time averaged order parameter r as

$$r = \lim_{\Delta t\to\infty} \frac{1}{\Delta t N} \int_{t_s}^{t_s+\Delta t} \left|\sum_{i=1}^{N} e^{i\varphi_i(t')}\right| dt',$$

Δt being a suitably long time interval, to be later specified. Furthermore, we denote by r_{ij} the time average of the pairwise synchronization between connected units, $r_{ij} = \lim_{\Delta t\to\infty} \frac{1}{\Delta t}\left|\int_{t_s}^{t_s+\Delta t} e^{i[\varphi_i(t')-\varphi_j(t')]} dt'\right|$, and define the local synchronization measure [9] as the ensemble average (over all N nodes) of the weighted average of r_{ij}

$$r_{\text{link}} = \frac{1}{N}\sum_{i=1}^{N}\sum_{j\in\mathcal{N}_i} w_{ij} r_{ij}.$$

Intuitively, this measure quantifies the average synchronization between connected nodes in the network. Even though both r and r_{link} are close to 0 (1) for very low (high) couplings, other dynamical regimes are observed where r_{link} is large while r is still small, corresponding to a high local synchrony before global order is obtained.

We consider a system with $N = 300$ and $K = 20$ and explore the structural and dynamical features as functions of λ and T. First, the system is integrated without adaptation (i.e., at fixed values of $w_{ij} = 1/K$) during 200 time units. Then, at an instant defined to be $t = 0$, the adaptation mechanism is activated; i.e., Eq. (2) is incorporated, and the network dynamics is integrated for another $t_s = 2000$ time units (such a period is at least 1 order of magnitude larger than that typically needed to reach the stationary state). Time t_s marks the beginning of the period of monitoring the global and local synchronization features in the network, which, in our simulations, is performed along an interval of $\Delta t = 1000$ time units [10]. Finally, all reported values result from a further ensemble average over 30 independent integrations of the system [11].

Figure 1(a) shows r as a function of λ and T. At relatively large values of T, r depends almost exclusively on λ, featuring a quasilinear dependence up to $\lambda \approx 4$, and

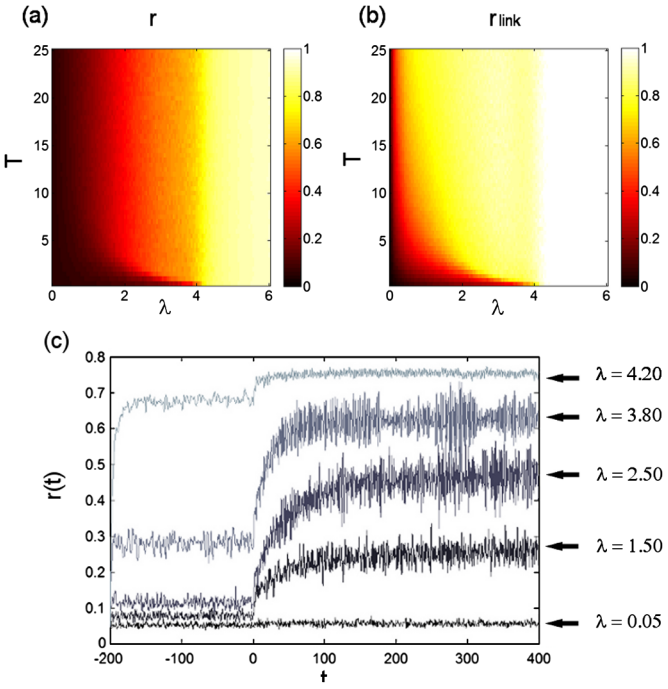


FIG. 1 (color online). Global and local synchronization indicators. r [(a), see text for definition] and r_{link} (b) in the (T, λ) parameter space. The color coding is reported in the right columns. (c) $r(t)$ for $T = 15$ and $\lambda \in \{0.05, 1.50, 2.50, 3.80, 4.20\}$ (specific values indicated by the arrows) for the nonadaptive ($t < 0$) and the adaptive ($t \geq 0$) evolution of the network.

then rising up steeply into its saturation plateau $r \sim 1$. This phase transition can be understood by referring to the classical Kuramoto model. Denoting, indeed, the natural frequency distribution by $g(\omega)$, the critical coupling of the Kuramoto model is $\lambda_c = 2/\pi g(0)$, which turns out to be 4 in our case [8]. We expect that, with increasing λ, a higher and higher synchronization level sets in the network, causing the p_{ij} to approach the value of 1. Thus, the w_{ij} will remain close to their initial value $1/K$ [see Eq. (2)]. At high enough λ, therefore, the system is almost indistinguishable from a modified Kuramoto model in which $N(N-1)/2 - NK$ links have been pruned. By monitoring $r(t)$ for $T = 15$ and several λ values [see Fig. 1(c)] one observes that $r(t)$ is already large at the preadaptive stage of the dynamics for λ close to λ_c. Figures 1(a) and 1(c) show that the adaptive mechanism has the effect of generically enhancing global synchronization in the network to a remarkable extent already for coupling strengths below the critical value.

Figure 1(b) shows r_{link} as a function of λ and T. For a given T, the local synchronization is a nonlinear, concave downwards function of λ, with, again, a sudden rise at $\lambda \approx \lambda_c$, that has the necessary amplitude to make r_{link} identically equal to one within our numerical accuracy. The growth of r_{link} with λ is, however, much faster than that of r, which delimits (for $\lambda < 1$ and $T > 1$) a wide region where the ratio r_{link}/r is always higher than 3 (and for the

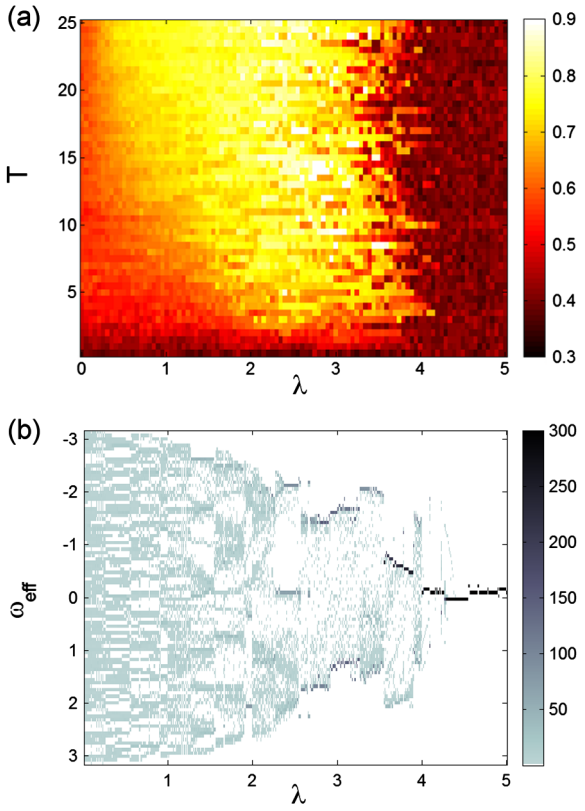


FIG. 2 (color online). Emergence of mesoscale structures. (a) MC (see text for definition) in the (T, λ) parameter space. The color coding is reported in the right column. (b) Distribution of the effective frequencies ω_{eff}, as a function of λ, for $T = 15$. The gray code (see column at the right of the panel) indicates the number of oscillators in the network displaying each specific value of ω_{eff}.

highest T and lowest λ values it can be even greater than 6), which is the hallmark of the emergence of modular (cluster) synchronization.

Further insight on such a modular structure can be obtained from Fig. 2, where we report [Fig. 2(a)] the modularity cohesion of the network in the parameter space, defined as

$$\text{MC} = \frac{\sum_{\mu=1}^{M} \sum_{i,j \in C_\mu} w_{ij}}{\sum_{\mu=1}^{M} \sum_{\nu=1}^{M} \sum_{i \in C_\mu, j \in C_\nu} w_{ij}} = \frac{1}{N} \sum_{\mu=1}^{M} \sum_{i,j \in C_\mu} w_{ij},$$

where C_μ runs over the M graph's communities (obtained by the optimization procedure described in [12] followed by the fast algorithm described in [13]). MC measures the fraction of the total network's wiring which is used to connect nodes belonging to the same community. It evaluates the degree of modularity of the partition, and takes values in [0, 1] (MC = 1 if the network is split into disconnected components). The striking result is that our network appears to be very well separated into components in the entire region where r is relatively low.

Figure 2(b) shows the distribution of the effective frequencies ω_{eff} (the average frequencies of the oscillators in the stationary regime) vs λ, for a typical realization using $T = 15$. Starting from the uniform distribution at $\lambda = 0$ (where ω_{eff} are all equal to the natural frequencies), increasing the coupling has the effect of producing a rich scenario of mesoscale patterns, forming different numbers of distinct synchronized communities at certain intervals of the λ axis. Eventually, at $\lambda \geq \lambda_c$, all oscillators coalesce into a single synchronous module.

This change in the modularity with increasing coupling strength is also reflected in the associated weight distribution (i.e., the topology resulting from the competitive adaptation mechanism), as demonstrated in Fig. 3 for $T = 15$. For $\lambda = 0.05$, there is no preferred scale and the bulk of the distribution seems to follow closely a power-law scaling, $p_{\hat{w}}(w) \propto w^{-\gamma}$ with $\gamma = 1.215 \pm 0.030$ [14]. In other words, adaptation produces here a complete

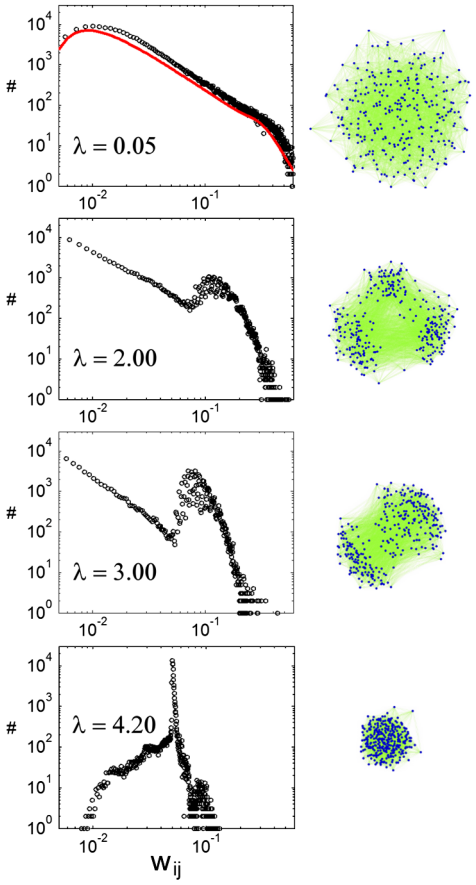


FIG. 3 (color online). Emergence of macroscale structures. (Left panels) Weight distribution for $T = 15$ and $\lambda \in \{0.05, 2.00, 3.00, 4.20\}$ (specific values indicated inside the plots). The red line in the upper plot ($\lambda = 0.05$) is the distribution of Eq. (4) calculated at $\lambda = 0$. (Right panels) Visual sketch of the corresponding network topologies, obtained by applying attractive forces between nodes proportional to the corresponding link weights.

redistribution of the weights, leading eventually to a highly heterogeneous topology. As λ increases, a local maximum appears in the distribution, and the network segregates into more and more distinct modules. The formation of three communities at $\lambda = 2$, and of two communities at $\lambda = 3$, have visible dynamical counterparts in Fig. 2(b). At large coupling strengths ($\lambda > \lambda_c$), the maximum is shifted toward $1/K = 0.05$ (i.e., the initial condition), and becomes more prominent. This is a direct consequence of the fact that for $\lambda > \lambda_c$ the network is able to synchronize even without adaptation [see Fig. 1(c)], and therefore the redistribution of weights is negligible.

The weight distribution can be derived analytically for $\lambda = 0$. It turns out, indeed, that this is useful for the estimation of the weight distribution not only for strictly vanishing λ, but also in the limit $\lambda \to 0$, as one could expect from heuristic continuity arguments. In such a case, the phases are uncoupled and evolve as $\varphi_i = \omega_i t + \varphi_i^0$. Plugging this evolution into Eq. (3), one obtains $p_{ij}^{(0)} = \frac{1}{\sqrt{1+[(\omega_i-\omega_j)T]^2}} = L(\omega_i - \omega_j)$, where the superscript in $p_{ij}^{(0)}$ highlights that we are in the uncoupled limit. Let us define $L(\Delta) = [1 + T^2\Delta^2]^{-1/2}$. This function takes values in [0, 1], and, as $L(\Delta) = L(-\Delta)$, it has no unique inverse. As in the uncoupled limit each node forms a closed subsystem with its neighbors, we can focus on the subsystem centered around a generic node i. Now, $\hat{\Delta}_j = \omega_j - \omega_i$ are independent identically distributed (i.i.d) random variables with conditioned probability density function (pdf) $p_{\hat{\Delta}_j}(\Delta_j|\omega_i)$ uniform in $[-\pi-\omega_i, \pi-\omega_i]$. All $L(\omega_i - \omega_j)$ such that $j \in \mathcal{N}_i$ are also i.i.d. random variables. We denote them by $\hat{L}_j$, and designate indistinctly as $L(\Delta_j)$ or L_j the values they take. The pdf of $\hat{L}_j$ conditioned on ω_i is

$$
\begin{aligned}
p_{\hat{L}_j}(L_j|\omega_i) &= \sum_{\Delta_j \in \{L_j^{-1}\}} \frac{1}{|\frac{dL_j}{d\Delta_j}|} p_{\hat{\Delta}_j}(\Delta_j|\omega_i) \\
&= \frac{\#\{\Delta | L(\Delta) = L_j\} \bigcap [-\pi - \omega_i, \pi - \omega_i]}{2\pi |L_j^2 T \sqrt{1 - L_j^2}|} \\
&= \frac{1}{2\pi |L_j^2 T \sqrt{1 - L_j^2}|} \\
&\quad \times \begin{cases} 0 & \text{if } L_j \geq 1 \\ 2 & \text{if } L(\pi - |\omega_i|) < L_j < 1 \\ 1 & \text{if } L(\pi + |\omega_i|) < L_j < L(\pi - |\omega_i|) \\ 0 & \text{if } L_j \leq L(\pi + |\omega_i|). \end{cases}
\end{aligned}
$$

The expectation value and the variance of L_j conditioned on ω_i are given by $\langle L_j(\omega_i)\rangle = \frac{1}{2\pi T}[\text{arcsinh}(T(-\pi - \omega_i)) + \text{arcsinh}(T(\pi + \omega_i))]$ and $\text{var}[L_j(\omega_i)] = \frac{1}{2\pi T}[\arctan(T(-\pi - \omega_i)) + \arctan(T(\pi + \omega_i))] - \langle L_j(\omega_i)\rangle^2$, respectively.

By Eq. (2), the weights have an asymptotic stable value given by $w_{ij}^{(0)} = \frac{p_{ij}^{(0)}}{\sum_{k\in\mathcal{N}_i} p_{ik}^{(0)}} = \frac{L_j}{L_j+G}$. Let us then define the random variable $\hat{G} = \sum_{k\in\mathcal{N}_i\setminus\{j\}} \hat{L}_k$. As both the expectation value and the variance of $\hat{L}_j$ are finite and independent of j, we invoke the central limit theorem for the sum in $\hat{G}$ and assert that it converges (in the limit of large K) to a Gaussian random variable with $\langle G\rangle = K\langle L_j(\omega_i)\rangle$, and $\text{var}[G] = K\text{var}[L_j(\omega_i)]$.

The pdf of $\hat{w}_{ij} = \hat{L}_j/(\hat{L}_j + \hat{G})$ conditioned on ω_i can be obtained by introducing the joint pdf for the independent variables $\hat{L}_j$ and $\hat{G}$: $p_{\hat{L}_j\hat{G}}(L_j, G|\omega_i) = p_{\hat{L}_j}(L_j|\omega_i)p_{\hat{G}}(G|\omega_i)$. By definition, $P(\hat{w}_{ij} < w_{ij} + \Delta w_{ij}) - P(\hat{w}_{ij}) = \int_\Omega p_{\hat{L}_j\hat{G}}(L_j, G|\omega_i)dL_j dG$, where $\Omega = \{(L, G)|w_{ij} \leq \frac{L_j}{L_j+G} \leq w_{ij} + \Delta w_{ij}\}$. This set can be reexpressed as $\{(L, G)|(\frac{1}{w_{ij}+\Delta w_{ij}} - 1)L \leq G \leq (\frac{1}{w_{ij}} - 1)L\}$. Such a parametrization allows one to rewrite

$$
\begin{aligned}
&P(\hat{w}_{ij} < w_{ij} + \Delta w_{ij}) - P(\hat{w}_{ij}) \\
&\quad = \int_0^1 dL_j \int_{(1/w_{ij}+\Delta w_{ij}-1)L_j}^{(1/w_{ij}-1)L_j} p_{\hat{L}_j\hat{G}}(L_j, G|\omega_i)dG \\
&\quad \approx \Delta w_{ij} \int_0^1 dL_j \frac{L_j}{w_{ij}^2} p_{\hat{L}_j}(L_j|\omega_i) p_{\hat{G}}\left(\left(\frac{1}{w_{ij}} - 1\right)L_j|\omega_i\right).
\end{aligned}
$$

As $p_{\hat{w}_{ij}}(w_{ij}|\omega_i) = \lim_{\Delta w_{ij}\to 0^+} \frac{P(\hat{w}_{ij} < w_{ij}+\Delta w_{ij}) - P(\hat{w}_{ij})}{\Delta w_{ij}}$, then one has

$$
\begin{aligned}
p_{\hat{w}_{ij}}(w_{ij}) &= \int_{-\infty}^{\infty} p_{\hat{w}_{ij}}(w_{ij}|\omega_i) p_{\hat{\omega}_i}(\omega_i) d\omega_i \\
&= \frac{1}{2\pi} \int_{-\pi}^{\pi} d\omega_i \int_0^1 dL_j \frac{L_j}{w_{ij}^2} p_{\hat{L}_j}(L_j|\omega_i) \\
&\quad \times p_{\hat{G}}\left(\left(\frac{1}{w_{ij}} - 1\right)L_j|\omega_i\right),
\end{aligned} \tag{4}
$$

which provides the analytic expression for the weight distribution in a generic closed subsystem, and thus in the whole network, at $\lambda = 0$. Figure 3 shows $p_{\hat{w}_{ij}}(w_{ij})$ (as a red continuous line) superimposed to the numerically obtained weight distribution for $\lambda = 0.05$. The fit is strikingly good, even though the central limit approximation for $K = 20$ is only mildly justified. Notice that the analytical curve in the uncoupled regime reproduces almost perfectly the numerical results for $\lambda = 0.05$, thus suggesting that Eq. (4) is a good approximation to the weight distribution in the regime of small λ.

In conclusion, we have shown how a network competitive adaptation leads to the emergence of those meso- and macroscale features which are commonly observed in real neural systems [15,16] and networks of social relations [17]. Our results indicate, therefore, that competitive

adaptation can be a general principle for the formation of heterogeneous structures in large ensembles of interacting units, with relatively segregated modules supporting highly synchronized dynamics.

Authors acknowledge the computational resources and assistance provided by CRESCO, the center of ENEA in Portici, Italy. A. A. is supported by Science Foundation Ireland (Grant No. 09/SIRG/I1615). J. G. G. is supported by Spanish MICINN through the Ramón y Cajal program and Projects No. FIS2008-01240 and No. MTM2009-13838.

[1] S. Boccaletti *et al.*, Phys. Rep. **424**, 175 (2006).
[2] D. O. Hebb, *The Organization of Behavior* (Wiley & Sons, New York, 1949).
[3] M. McPherson, L. Smith-Lovin, and J. M. Cook, Annu. Rev. Sociol. **27**, 415 (2001).
[4] G. G. Turrigiano and S. B. Nelson, Nat. Rev. Neurosci. **5**, 97 (2004).
[5] R. I. M. Dunbar, J. Hum. Evol. **22**, 469 (1992).
[6] T. Nowotny *et al.*, J. Neurosci. **23**, 9776 (2003).
[7] P. Seliger, S. C. Young, and L. S. Tsimring, Phys. Rev. E **65**, 041906 (2002).
[8] Y. Kuramoto, *Chemical Oscillations, Waves and Turbulence* (Springer, New York, 1984).
[9] J. Gómez-Gardeñes, Y. Moreno, and A. Arenas, Phys. Rev. Lett. **98**, 034101 (2007).
[10] Systematic checkings indicate that r and r_{link} are not appreciably altered by increasing Δt gradually up to 2000 time units (changes only very rarely exceed 1%, and are generally orders of magnitude smaller).
[11] The integration is performed with a 4th order Runge-Kutta algorithm, at 0.02 integration time step.
[12] J. Duch and A. Arenas, Phys. Rev. E **72**, 027104 (2005).
[13] M. E. J. Newman, Phys. Rev. E **69**, 066133 (2004).
[14] The exponent comes from a power-law fit based on the nonlinear least-squares Newton-Gauss algorithm.
[15] V. M. Eguíluz *et al.*, Phys. Rev. Lett. **94**, 018102 (2005).
[16] D. Meunier, R. Lambiotte, and E. T. Bullmore, Front. Neurosci. **4**, 200 (2010); M. Chavez *et al.*, Phys. Rev. Lett. **104**, 118701 (2010).
[17] J. Scott, *Social Network Analysis: A Handbook* (Sage Publications, London, 2000), 2nd ed.; F. Liljeros *et al.*, Nature (London) **411**, 907 (2001).